Barrier-free absorbance modulation for super-resolution optical lithography

Apratim Majumder,[1] Farhana Masid,[1] Benjamin Pollock,[2] Trisha L. Andrew,[2] and Rajesh Menon[1,*]

[1]*Department of Electrical and Computer Engineering, University of Utah, Salt Lake City, UT 84102, USA*
[2]*Department of Chemistry, University of Wisconsin-Madison, Madison, WI 53706, USA*
[*]*rmenon@eng.utah.edu*

Abstract: Absorbance-Modulation-Optical Lithography (AMOL) enables super-resolution optical lithography by simultaneous illumination of a photochromic film by a bright spot at one wavelength, λ_1 and a node at another wavelength, λ_2. A deep subwavelength region of the transparent photochromic isomer is created in the vicinity of the node. Light at λ_1 penetrates this region and exposes an underlying photoresist layer. In conventional AMOL, a barrier layer is required to protect the photoresist from the photochromic layer. Here, we demonstrate barrier-free AMOL, which considerably simplifies the process. Specifically, we pattern lines as small as 70nm using λ_1 = 325nm and λ_2 = 647nm. We further elucidate the minimum requirements for AMOL to enable multiple exposures so as to break the diffraction limit.

References and links

1. F. M. Scellenberg, "Selected papers on resolution enhancement techniques in optical lithography," SPIE Milestone Services **178**, (2004).
2. E. Abbé, "Beitragezurtheorie des mikroskops und der mikroskopischenwahrnehmung," Arch. Mikrosk. Anat. Entwichlungsmech **9**(1), 413–418 (1873).
3. E. A. Ash and G. Nicholls, "Super-resolution aperture scanning microscope," Nature **237**(5357), 510–512 (1972).
4. E. Betzig, J. K. Trautman, T. D. Harris, J. S. Weiner, and R. L. Kostelak, "Breaking the diffraction barrier: optical microscopy on a nanometric scale," Science **251**(5000), 1468–1470 (1991).
5. L. Novotny, B. Hecht, and D. Pohl, "Implications of high resolution to near-field optical microscopy," Ultramicroscopy **71**(1–4), 341–344 (1998).
6. S. W. Hell and J. Wichmann, "Breaking the diffraction resolution limit by stimulated emission: stimulated-emission-depletion fluorescence microscopy," Opt. Lett. **19**(11), 780–782 (1994).
7. J. T. Fourkas, "Nanoscale photolithography with visible light," J. Phys. Chem. Lett. **1**(8), 1221–1227 (2010).
8. L. Li, R. R. Gattass, E. Gershgoren, H. Hwang, and J. T. Fourkas, "Achieving lambda/20 resolution by one-color initiation and deactivation of polymerization," Science **324**(5929), 910–913 (2009).
9. T. F. Scott, B. A. Kowalski, A. C. Sullivan, C. N. Bowman, and R. R. McLeod, "Two-color single-Photon photoinitiation and photoinhibition for subdiffraction photolithography," Science **324**(5929), 913–917 (2009).
10. T. Tsuujioka, M. Kume, Y. Horikawa, A. Ishikawa, and M. Irie, "Super-resolution disk with a photochromic mask layer," Jpn. J. Appl. Phys. **36**(Part 1, No. 1B), 526–529 (1997).
11. T. Tsujioka, M. Kume, and M. Irie, "Theoretical analysis of super-resolution optical disk mastering using a photoreactive dye mask layer," Opt. Rev. **4**(3), 385–389 (1997).
12. J. Fischer, G. von Freymann, and M. Wegener, "The materials challenge in diffraction-unlimited direct-laser-writing optical lithography," Adv. Mater. **22**(32), 3578–3582 (2010).
13. R. Wollhofen, J. Katzmann, C. Hrelescu, J. Jacak, and T. A. Klar, "120 nm resolution and 55 nm structure size in STED-lithography," Opt. Express **21**(9), 10831–10840 (2013).
14. Z. Gan, Y. Cao, R. A. Evans, and M. Gu, "Three-dimensional deep sub-diffraction optical beam lithography with 9 nm feature size," Nat. Commun. **4**(2061), 2061 (2013).
15. C. Fonseca, M. Somervell, S. Scheer, Y. Kuwahara, K. Nafus, R. Gronheid, S. Tarutani, and Y. Enomoto, "Advances in dual-tone development for pitch frequency doubling," Proc. SPIE **7640**, 76400E (2010).

16. R. Menon and H. I. Smith, "Absorbance-modulation optical lithography," J. Opt. Soc. Am. A **23**(9), 2290–2294 (2006).
17. T. L. Andrew, H.-Y. Tsai, and R. Menon, "Confining light to deep subwavelength dimensions to enable optical Nanopatterning," Science **324**(5929), 917–921 (2009).
18. F. Masid, T. L. Andrew, and R. Menon, "Optical patterning of features with spacing below the far-field diffraction limit using absorbance modulation," Opt. Express **21**(4), 5209–5214 (2013).
19. G. Pariani, R. Castagna, R. Menon, C. Bertarelli, and A. Bianco, "Modeling absorbance-modulation optical lithography in photochromic films," Opt. Lett. **38**(16), 3024–3027 (2013).
20. J. Foulkes and R. Blaikie, "Finite Element Simulation of Absorbance Modulation Optical Lithography," in *Proceedings of International Conference on Nanoscience and Nanotechnology (ICONN 2008)*, 184–187 (2008).
21. R. Menon, D. Gil, and H. I. Smith, "Experimental characterization of focusing by high-numerical-aperture zone plates," J. Opt. Soc. Am. A **23**(3), 567–571 (2006).
22. T. Ito, T. Yamada, Y. Inao, T. Yamaguchi, N. Mizutani, and R. Kuroda, "Fabrication of half-pitch 32 nm resist patterns using near-field lithography with a - Si mask," Appl. Phys. Lett. **89**(3), 033113 (2006).

1. Introduction

The capability of the semiconductor industry to continuously produce nano-scale patterns using conventional top-down photolithography is fast approaching its limits due to diffraction. Scaling the exposure wavelength to extreme ultraviolet (EUV, λ~13nm) is the industry-chosen approach for next-generation lithography. However, it is increasingly clear that this solution is considerably more expensive and does not provide sufficient throughput for many applications [1]. Resolution in photolithography is fundamentally limited by the diffraction limit to about λ/2, where λ is the illumination wavelength [2]. If one were able to circumvent this limit, inexpensive and mature long-wavelength sources and concomitant processes can be used for advanced lithography. Near-field-optical lithography has been proposed to overcome this limit by localizing the illumination to sub-wavelength regions [3–5]. However, the feature-size control for these techniques is fraught with problems, since the gap between the photomask and the photoresist needs to be controlled to nanometer precision over the field of exposure (several mm^2). An alternative and more promising approach exploits reversible photochemical transitions inspired by successes in stimulated-emission-depletion-microscopy (STED) [6]. In particular, these employ either a combination of 2-photon polymerization and 1-photon de-polymerization [7, 8] or single-photon photo-initiation-photo-inhibition [9] to drastically suppress the vicinity of a region where exposure occurs. Techniques that can separate the photo-switching element from the recording media [10, 11] have also been proposed. For all of these techniques, several materials challenges exist [12]. In addition to the ability to fabricate isolated structures with feature sizes below the diffraction limit, it must be realized that breaking the far-field diffraction limit requires patterning two neighboring features separated by a distance that is less than λ/2. There are examples of two-photon direct laser writing combined with STED lithography [13] that have been able to achieve a separation of 52nm between two lines [14]. However these processes involve very high intensities for the two-photon polymerization step, specialized resins and polymers, pulsed laser systems that are expensive, and also are relatively slow. In the semiconductor industry, multiple patterning is used to achieve sub-wavelength resolution. However, this involves an etching step after each exposure, which considerably reduces throughput, increases processing steps and requires precise overlay. Another option is to manipulate the chemical formulation of the photoresist to increase its nonlinearity or to enable dual-tone development [15].

Our approach, named Absorbance-Modulation-Optical Lithography (AMOL) [16] was able to pattern features with widths less than 1/10th of the exposure wavelength [17]. AMOL uses a thin photochromic film referred to as the Absorbance-Modulation Layer (AML) that is simultaneously illuminated with a writing beam focused to a spot of wavelength, λ_1 and a confining beam focused to a ring of wavelength, λ_2. λ_1 is typically in the UV region (325 nm) and converts the AML to a transparent form (transparent to λ_1), while λ_2, a visible wavelength reverses the reaction to render the AML opaque (opaque to λ_1). These competing effects restrict the transmission of λ_1 to the vicinity of the nodes of λ_2. A photoresist layer placed

below the AML records the λ_1 photons. Since the region through which λ_1 can penetrate the AML is primarily limited not by diffraction but by the photochemical equilibrium, the diffraction limit can be overcome. Thus the advantages of AMOL are: (a) it involves no intermittent etch step, (b) the non-linearity is introduced within the AML and hence, subsequent exposures can be spaced at separations less than the diffraction limit, (c) no chemical re-formulation of photoresist is required – one of the important points of this article is to show the compatibility of the AMOL process and the AML material formulation with commercially available photoresist in order to prove that AMOL can be easily adapted to current technologies and (d) no high light intensities are required.

In previous implementations of AMOL, a barrier layer (typically poly-vinyl alcohol or PVA) is utilized to protect the photoresist from the solvents used to spin-cast the AML. This barrier layer has to be thick enough to protect the photoresist but thin enough to prevent significant diffraction of the transmitted λ_1 photons. Furthermore, this layer has to be removed after exposure and prior to development of the photoresist. It would be extremely useful to develop a technique, where this barrier layer isn't necessary. Recently, a method was proposed to invert the sample stack to remove this barrier layer [18]. However, this method is only applicable for transparent samples and is not useful for silicon.

In this article, we present three important contributions. Firstly, we demonstrate barrier-free AMOL. Secondly, we validate previous numerical predictions of scaling of the feature size with the ratio of the peak intensities at λ_1 and at λ_2 [19, 20]. Thirdly, we elucidate the process requirements to allow AMOL to break the diffraction limit by enabling multiple exposures of closely spaced features.

2. Experiments

We developed a formulation of the AML that is chemically compatible with two conventional photoresists. The AML was formulated using the photochromic molecule 1,2-bis(5,5′ – dimethyl-2,2'-bithiophen-4-yl) perfluorocyclopent-1-ene (otherwise referred to as BTE) suspended in a polymer-matrix of polystyrene dissolved in Toluene with a 93.63% loading of the BTE in the solution. The photoresists used were the S1813 resist from Shipley and M91Y, a chemically amplified photoresist from JSR Micro. Both resists were extensively tested against toluene over extended periods (several hours) and was shown to have no deleterious impact.

The apparatus used to conduct the lithographic exposures for AMOL is illustrated in Fig. 1. We used a modified Mach-Zehnder interferometer (MZI), shown in Fig. 1(a) to expose our samples. The MZI consisted of the λ_2 (647 nm) laser beam being spatially filtered, collimated and then split by a beam-splitter, guided by mirrors and re-combined at the sample to generate a standing wave. The λ_1 (325 nm) beam was also spatially filtered, collimated and allowed to uniformly illuminate the sample. The AML of the sample was therefore illuminated by a standing wave at λ_2 and a uniform illumination at λ_1. This allowed for the regions of the AML that coincident with the nodes of the λ_2 standing wave to remain transparent, enabling a sub-wavelength exposure of the underlying photoresist. It may be noted that Fig. 1 is a simple illustration to demonstrate the barrier-layer free AMOL process and the diagrammatic representation of the light intensity inside the depth of the photoresist layer and the AML are not strictly accurate. The figure is for illustrative purposes only, as the aim of this article is primarily focused at demonstrating the barrier-free AMOL process and the line-width scaling and accurate AMOL models exist in literature [19, 20].
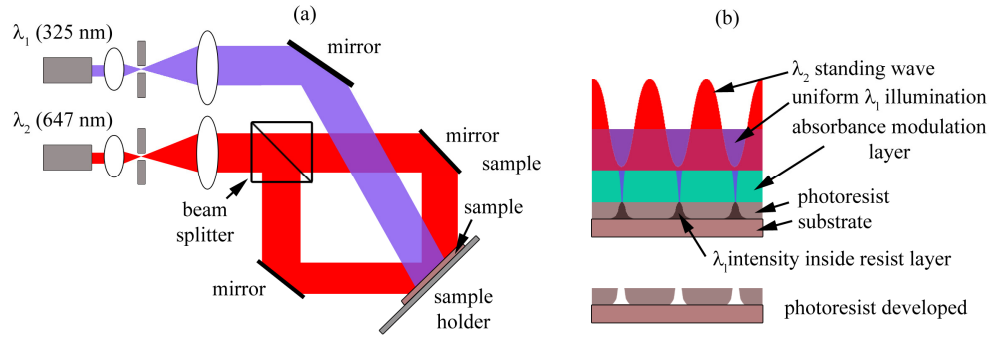
Fig. 1. Experimental set-up to perform AMOL. (a) Schematic of the modified Mach-Zehnder interferometer. Light at λ_2 = 647nm interferes with itself to produce a standing wave while light at λ_1 = 325nm uniformly illuminates the sample. The period of the λ_2 standing wave is 457nm. (b) The sample stack is illuminated by a standing wave at λ_2 and a uniform illumination at λ_1. The competing action of both wavelengths through the absorbance modulation layer exposes the photoresist.

2.1 Linewidth scaling

The silicon wafer substrates were RCA1 and Piranha cleaned and then spin-coated first with a monolayer of hexamethyldisilazane (HMDS) at 6000RPM for 60s with immediate application of the photoresist. Shipley 1813, pre-diluted using Propylene glycol monomethyl ether acetate in the ratio 1:5 by weight, was spun at 4500RPM for 60s with subsequent baking on a hot plate at 115°C for 60s to create a ~500nm-thick layer. Lastly the AML was spin-coated on top of the resist at 730RPM for 60s with subsequent air-drying for 10 minutes, resulting in a thickness of ~650 nm. An illustration of the sample stack is shown in Fig. 1(b). After exposure, the AML was stripped by vigorously rinsing in Toluene for 15s followed by blowing with dry N_2. Dipping in Microposit MF 325 developer for 60 s developed the Shipley 1813 photoresist. Finally, the sample was sputter coated with a thin layer (3-4 nm) of Au/Pd alloy using a Gatan 682 PECS desktop sputter system for inspection in a scanning-electron microscope (FEI Quanta 600 FE-ESEM).

One of the most important features of AMOL is the dependence of the linewidth on the ratio of the peak-intensities of the two wavelengths, instead of the absolute value of the intensity of either [17]. We mapped the line-spread function (LSF) that is recorded in the photoresist (illustrated by circles in Fig. 2(a)) following a previously described technique [21]. Exposures were carried out at four different peak-intensity ratios (I_2/I_1): 2000, 1000, 500 and 100. For each of these ratios, the linewidth is plotted with respect to the inverse of the normalized dose, as shown in Fig. 2(a). We can clearly see that the LSF gets constricted as the ratio is increased. Scanning electron micrographs of the fabricated lines are also shown in Fig. 2(b). The smallest lines resolved are around 90 nm, which is equivalent to $\lambda_1/3.6$ and $\lambda_2/7.2$, respectively. Note that the spacing between the lines is determined by the period of the λ_2 standing wave.
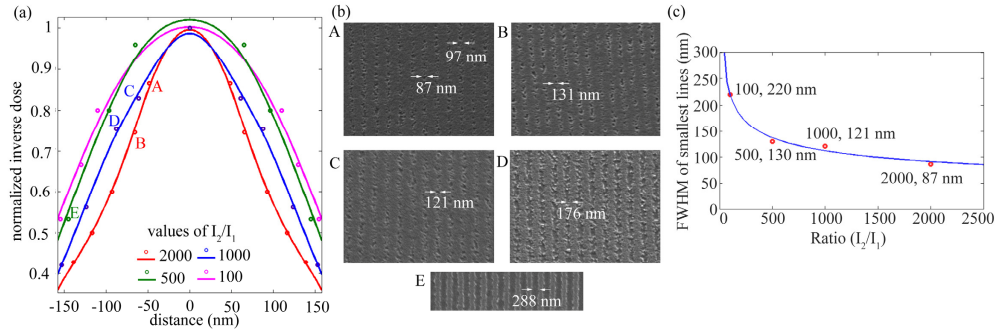
Fig. 2. (a) Mapping of the line-spread function (LSF) for different values of the intensity ratio I_2/I_1. The circles represent the actual exposure results while the solid lines are fits to sinusoids using smoothing spline method. (b) Scanning electron micrographs of the fabricated lines whose measurements were used as the data for the plot shown in part (a). (c) Plot of the FWHM (Full-Width at Half-Maximum) of the smallest lines obtained for each ratio versus the intensity ratio shows the line-width scaling property of AMOL as a function of the intensity ratio of the two wavelengths.

2.2 Conditions for breaking the diffraction limit

In order for AMOL to overcome the diffraction limit, we need to pattern two neighboring features, whose spacing is less than $\lambda/2$. This can be achieved by enabling the AML to recover to its original opaque form everywhere after the first feature has been exposed. Subsequently, the sample is displaced and the second feature is patterned. This process has been described previously [17]. However, for this process to work properly, we need to ensure that the AML recovers adequately to its original opaque state. It also requires that the background exposure from λ_1 during each exposure step is minimized. We can refer to this as the contrast of the AML during exposure. This contrast is nonlinearly dependent upon the ratio of peak intensities (I_2/I_1). The question we wanted to answer was, what the minimum ratio, I_2/I_1 is, that is required to enable sufficient contrast in order to overcome the diffraction limit. To answer this question, we performed of UV-Vis absorbance spectroscopy on transparent (fused silica) samples coated with the AML that were exposed to varying ratios I_2/I_1. The results are plotted in Fig. 3.

The samples were first treated with a monolayer of hexamethyldisilazane (HMDS) followed by application of the AML, spin-coated at 730RPM for 60s with subsequent air-drying, for a 650 nm layer. One sample was exposed to uniform λ_1 and λ_2 simultaneously at an I_2/I_1 ratio of ~1000, and its UV-Vis absorbance spectra was monitored after 30min, 60min and 90min of exposure time. Any change in the absorbance spectrum indicates that the photo-stationary state has not been reached, which implies that the ratio (and the contrast) is not high enough. As seen in Fig. 3(a), the absorbance at 325nm reduces with increased exposure time. This means that the opacity of the AML to λ_1 at this ratio (1000) decreases and hence, would contribute to a UV background illumination for the photoresist. This experiment was repeated with $I_2/I_1 = 4000$, and absorbance spectra were taken after 60min and 240min of exposure. As seen in Fig. 3(b), there is no change in the absorbance at 325nm. The absorbance for the 2 samples is plotted as a function of time in Fig. 3(c). It is clear that with $I_2/I_1 = 4000$, one can avoid any background exposure of the photoresist.
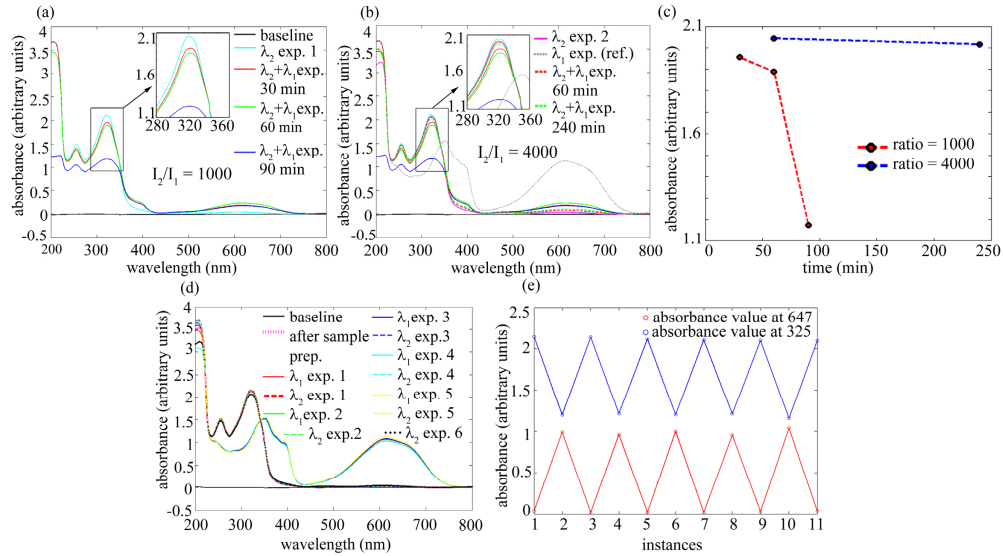
Fig. 3. UV-Vis measurements of the AML layer after simultaneous exposure to the two wavelengths at (a) 1000 intensity ratio, shows the decrease in the opacity of the AML to λ_1, but (b) at 4000 intensity ratio – shows that the opacity of the AML to the λ_1 wavelength is retained. (c) Comparison of the absorbance of the AML at 325 nm for different ratios of simultaneous exposures to λ_1 and λ_2. (d) UV-Vis measurements to show the photo-switch-ability of the AML layer. (e) Absorbance values at the λ_1 and λ_2 wavelengths show that the opacity of the AML layer to λ_1 can be recovered repeatedly.

Another important metric for the AML is its ability to switch between the opaque and transparent states multiple times without any degradation in its absorbance. We monitored the absorbance spectra, while exposing the transparent sample to uniform λ_1 (325nm) illumination at 200μW for 30min (dose approximately equal to the lithographic single exposure dose) and then to uniform λ_2 (647nm) illumination at 200mW for 90min (dose approximately equal to the AML recovery step dose). This is done about 6 times, mimicking 6 exposures. The results plotted in Figs. 3(d) and 3(e) indicate that the AML is indeed able to photo-switch in a repeatable and stable manner.

2.3 Barrier-free AMOL

In order to demonstrate the efficacy of barrier-free AMOL, we built a somewhat simpler Lloyd's-mirror-based interferometer system as illustrated in Fig. 4(a). Lines patterned in S1813 at an intensity ratio (I_2/I_1) = 4000 with an average line-width of ~84 nm are shown in Fig. 4(b). In order to overcome the low sensitivity of the S1813 photoresist, we also developed a process utilizing M91Y, a chemically-amplified resist (CAR) from JSR Micro. This photoresist was sensitized to 325 nm by adding CGI 725 sensitizer (BASF) in the ratio 51:1 by weight. We further verified that this resist is also compatible with toluene, the solvent used for spin-casting the AML. The sensitized M91Y was spun at 6000 RPM for 60s with subsequent baking at 130°C for 90s to create a 450 nm-thick layer. After exposure, the AML layer was first removed by dipping the sample in Toluene for 15 s, then the sample was baked on a hot plate at 130°C for 90 s before being developed in Microposit MF CD-26 developer (0.26N tetramethylammonium hydroxide) for 60s. The sensitized M91Y photoresist has much higher sensitivity than S1813 and also demonstrates significantly lower line-edge roughness as seen by the scanning-electron micrographs in Figs. 4(c). Here, we show lines as thin as 70nm at an intensity ratio of 4000, which is equivalent to $\lambda_1/4.6$ and $\lambda_2/9.2$, respectively. Note that in all cases, no barrier is utilized between the AML and the photoresist.
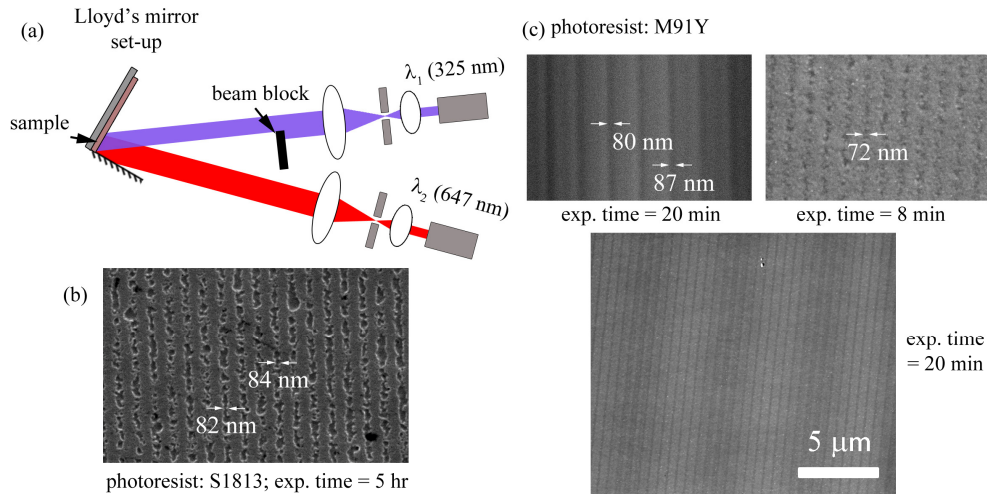
Fig. 4. (a) Modified Lloyd's mirror interferometer for proof-of-principle AMOL exposures. (b) Lines of width ~80 nm fabricated in S1813 photoresist at an intensity ratio of 4000. (c) Lines of width ~70-80nm created in sensitized M91Y photoresist at an intensity ratio of 4000.

It may be noted that the photoresist layer thickness (450-500 nm) is large compared to the achieved linewidths (~70 nm) and this depth will allow for the light at λ_1 to diffract into the depth of the resist layer, with considerable lateral spread. Hence it is evident that in order to fully realize the potential of AMOL and faithfully record the high spatial frequencies in the near-field, ultra-thin photoresist layers are required which agrees well with established literature [22].

3. Conclusion

Here, we demonstrated an approach for optical-super-resolution nanolithography that utilizes an absorbance-modulation layer that is placed directly atop the photoresist layer. By removing the barrier layer that is typically used, we have simplified the lithographic process. Secondly, we utilized this process to demonstrate that the width of an exposed line scales as the ratio of the peak intensities at the nodal and the writing wavelengths. Finally, we performed careful UV-Vis absorbance spectroscopy studies to elucidate the minimum contrast requirements of the AML so as to overcome the diffraction limit via multiple exposures. Combining these advancements with further process optimization will allow for a maskless optical nanopatterning technique that is not only scalable (fast) but also can achieve deep subwavelength resolutions.

Acknowledgment